ACS chemical biology

Articles

Cite This: ACS Chem. Biol. 2019, 14, 2286−2294

pubs.acs.org/acschemicalbiology

Membrane Disruption by Very Long Chain Fatty Acids during Necroptosis

Laura R. Parisi,[†] Shahin Sowlati-Hashjin,[‡,⊥] Ilyas A. Berhane,[†] Samuel L. Galster,[†] Kevin A. Carter,[∥] Jonathan F. Lovell,[∥] Sherry R. Chemler,[†] Mikko Karttunen,[‡,§,⊥] and G. Ekin Atilla-Gokcumen*[,†]

[†]Department of Chemistry, University at Buffalo, The State University of New York, Buffalo, New York 14260, United States

[‡]Department of Chemistry, The University of Western Ontario, 1151 Richmond Street, London, Ontario N6A 5B7, Canada

[§]Department of Applied Mathematics, The University of Western Ontario, 1151 Richmond Street, London, Ontario N6A 5B7, Canada

[∥]Department of Biomedical Engineering, University at Buffalo, The State University of New York, Buffalo, New York 14260, United States

[⊥]The Centre of Advanced Materials and Biomaterials Research, The University of Western Ontario, 1151 Richmond Street, London, Ontario N6A 5B7, Canada

Supporting Information

ABSTRACT: Necroptosis is a form of regulated cell death which results in loss of plasma membrane integrity, release of intracellular contents, and an associated inflammatory response. We previously found that saturated very long chain fatty acids (VLCFAs), which contain ≥20 carbons, accumulate during necroptosis. Here, we show that genetic knockdown of Fatty Acid (FA) Elongase 7 (ELOVL7) reduces accumulation of specific very long chain FAs during necroptosis, resulting in reduced necroptotic cell death and membrane permeabilization. Conversely, increasing the expression of ELOVL7 increases very long chain fatty acids and membrane permeabilization. *In vitro*, introduction of the VLCFA C24 FA disrupts bilayer integrity in liposomes to a greater extent than a conventional C16 FA. To investigate the microscopic origin of these observations, atomistic Molecular Dynamics (MD) simulations were performed. MD simulations suggest that fatty acids cause clear differences in bilayers based on length and that it is the interdigitation of C24 FA between the individual leaflets that results in disorder in the region and, consequently, membrane disruption. We synthesized clickable VLCFA analogs and observed that many proteins were acylated by VLCFAs during necroptosis. Taken together, these results confirm the active role of VLCFAs during necroptosis and point to multiple potential mechanisms of membrane disruption including direct permeabilization via bilayer disruption and permeabilization by targeting of proteins to cellular membranes by fatty acylation.

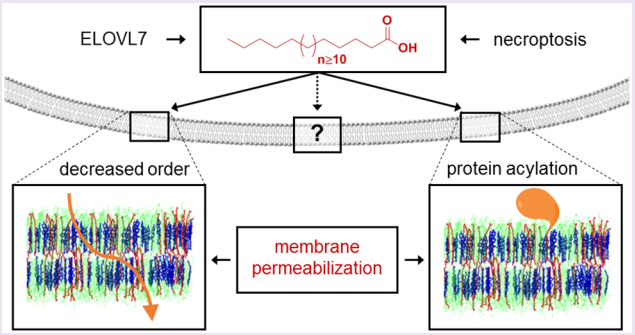

Lipids have many significant roles in maintaining cellular homeostasis.[1] In addition to forming the essential permeability barriers of cells, lipids actively participate in numerous cellular processes,[2] and lipid dysfunction is closely linked to human pathologies.[3,4] Cells maintain complex networks of pathways consisting of hundreds of different enzymes that are involved in the biosynthesis of thousands of unique lipid species.[5] We have only recently begun to understand and appreciate how structural specificity within a given lipid family (i.e., alkyl chain length and degree of unsaturation) impacts lipid function.[6−8]

Fatty acids are among the simplest lipids. The mammalian fatty acid repertoire consists of linear alkyl chains with various degrees of unsaturation. Palmitic acid, which contains a saturated C16 alkyl chain, is the major product of *de novo* fatty acid biosynthesis, which can be elongated and desaturated by the concerted action of elongases and desaturases.[9]

Fatty acids are building blocks for complex lipid structures and can act as signaling lipids through their covalent modification of proteins. This process, protein fatty acylation, controls subcellular localization of cytoplasmic proteins to the cellular membranes (reviewed in refs 10, 11). Recent studies have uncovered novel exciting findings on the role of distinct fatty acids in different cellular processes. For instance, the degree of unsaturation of fatty acids can modulate how cells respond to cellular stress, especially when linked to lipid oxidation.[12,13] Similarly to degrees of unsaturation, the alkyl chain length has been shown to be important for toxicity in neurons[14] and affect the biophysical properties of organelle membranes.[15]

Received: July 31, 2019
Accepted: September 6, 2019
Published: September 6, 2019

DOI: 10.1021/acschembio.9b00616
ACS Chem. Biol. 2019, 14, 2286−2294

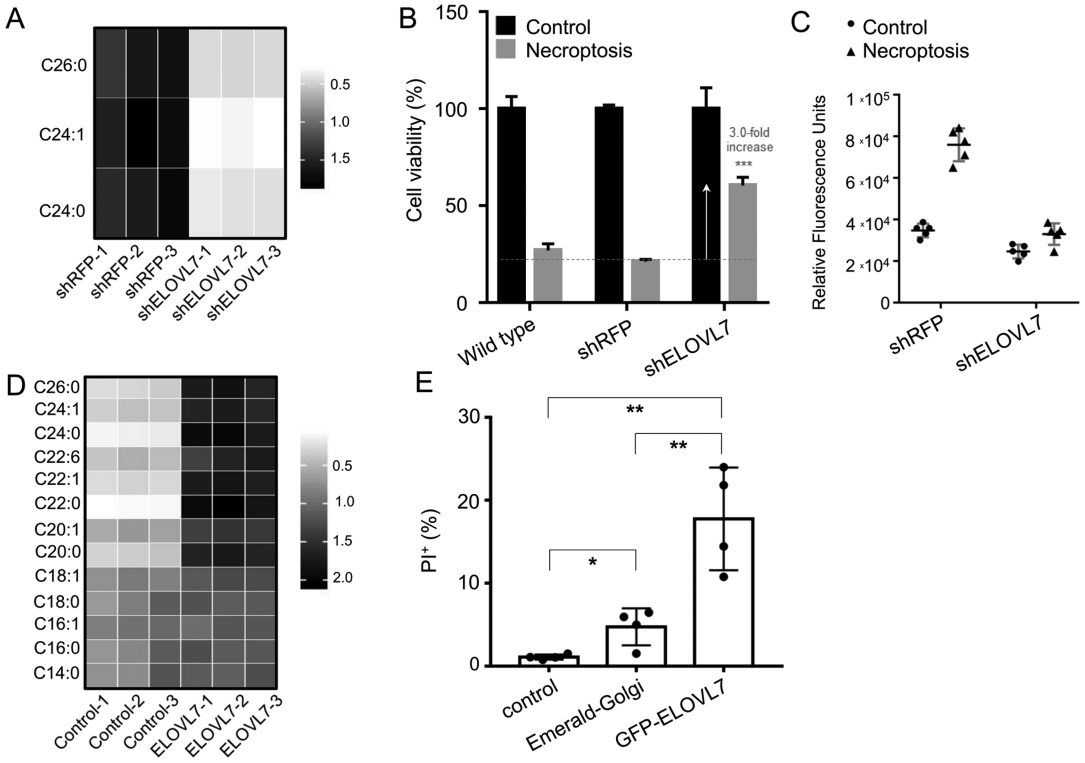

Figure 1. ELOVL7 regulation of VLCFA levels and membrane integrity. (A) ELOVL7 knockdown decreases VLCFA levels in necroptotic cells. Heatmap depicts the relative abundance of VLCFAs during necroptosis in HT-29 cells transduced with shRFP or shELOVL7. Relative abundance is calculated by dividing the abundance of a lipid by the average abundance of that lipid in the compared samples. (B) ELOVL7 knockdown reduces necroptotic cell death. Relative viability of wild type, shRFP, and shELOVL7 transduced cells treated with BV6/zVAD-FMK/TNF-alpha to induce necroptosis compared to vehicle-treated control cells. Error bars represent 1 SD; $n = 5$. ***$p < 0.001$. (C) ELOVL7 knockdown prevents necroptotic membrane permeabilization. shRFP and shELOVL7 cells were treated with vehicle or BV6/zVAD-FMK/TNF-alpha to induce necroptosis. PI uptake was measured by relative fluorescence. The horizontal black lines indicate the mean of $n = 5$ replicates per condition; gray error bars represent ±1 SD. (D) ELOVL7 overexpression increases VLCFA levels. Heatmap depicts the relative abundance of fatty acids in HEK-293T cells which were transiently transfected to overexpress ELOVL7-GFP and mock-transfected controls. (E) ELOVL7 overexpression compromises membrane integrity. PI^+ HEK-293T cell populations were determined in untransfected control cells, cells transfected for 48 h to overexpress GFP-ELOVL7, and cells transfected for 48 h to overexpress the Emerald-Golgi protein as an additional control. PI^+ populations were determined as a percent of the total cell population for untransfected control cells and as a percent of the GFP^+ or $Emerald^+$ cell populations for transfected cells. Error bars represent ±1 SD; $n = 4$. *$p < 0.05$, **$p < 0.01$.

We recently conducted the first untargeted lipidomic analysis of necroptotic cells and identified lipid participants of this process.[16] Necroptosis is a form of regulated cell death that exhibits phenotypic hallmarks of necrotic cell death including cell and organelle swelling and the permeabilization of cellular membranes upon activation of the death pathway.[17] The permeabilization of the plasma membrane, in particular, results in the release of cytokines and other molecules to the extracellular matrix, which can result in an inflammatory response at the organismal level.[18,19] In an effort to identify lipids involved in membrane permeabilization during necroptosis, we analyzed the changes in lipid composition in multiple cell lines during this process. We focused on necroptosis-specific changes in the cellular lipidome and identified accumulations of saturated very long chain fatty acids (VLCFAs) as the most profound and significant changes that occur during necroptosis. We found that inactivation of fatty acid synthase (the enzyme that is responsible for the synthesis of C16 FA) resulted in increased cell viability and prevented the loss of plasma membrane integrity during this process. These results strongly suggested that VLCFAs are involved in necroptosis.[16]

In this work, we study the involvement of VLCFAs during necroptosis. We show that depleting the levels of VLCFAs that specifically accumulate during necroptosis by suppressing Fatty Acid Elongase 7 (ELOVL7) activity prevents membrane permeabilization and results in a significant increase in cell viability during necroptosis. Overexpression of ELOVL7 causes accumulation of VLCFAs and permeabilizes the plasma membrane. Combined, these results suggest that VLCFAs might affect membrane integrity. Based on this, we next studied the interaction of C16 FA and C24 FA with lipid bilayers in liposomes and using Molecular Dynamics (MD) simulations. We found that C24 FA can disturb membrane integrity more readily than C16 FA. MD simulations show that C24 FA can interdigitate between leaflets of the lipid bilayer, whereas C16 FA does not. Finally, we show that a representative VLCFA, C20 FA, can covalently modify a number of proteins during necroptosis. Overall, our results support a model where increases in the levels of saturated VLCFAs result in cellular membrane permeabilization during necroptosis. Our model also supports that, at the membrane level, VLCFAs can cause membrane disruption either by directly disrupting membrane packing or facilitating permeabilization by targeting proteins to the plasma membrane.

DOI: 10.1021/acschembio.9b00616
ACS Chem. Biol. 2019, 14, 2286−2294

RESULTS

Knockdown of ELOVL7 Ameliorates Necroptotic Cell Death. Our previous work has shown that VLCFAs increase significantly during necroptosis, and that treatment with cerulenin, a small molecule fatty acid analog that prevents VLCFA accumulation, significantly ameliorates necroptotic cell death and membrane permeabilization. We also showed that inactivation of fatty acid synthase (FASN) prevents VLCFA accumulation and significantly diminishes cell death during necroptosis.[16]

In order to further establish that these protective effects result from blocking the accumulation of VLCFA, we wanted to interrogate the role of fatty acid elongation during necroptosis. Fatty acid elongation is carried out by the action of multiple enzymes. Elongation of very long chain fatty acids proteins (ELOVLs) catalyze the rate-limiting step of long/very long chain fatty acid elongation. There are seven isoforms with different substrate specificities based on alkyl chain structure.[20] ELOVL1 and ELOVL7 have both been associated with the production of saturated VLCFA,[21,22] and our previous work demonstrated that ELOVL1 and -7 show 2.7- and 6-fold upregulation during necroptosis.[16] We decided to focus on ELOVL7 based on its profound and significant activation during necroptosis. We inactivated ELOVL7 in HT-29 cells using shRNA (referred to as shELOVL7) and investigated the sensitivity of shELOVL7 cells toward necroptotic stimuli as compared to shRFP as a negative control. We found that shELOVL7 cells had significantly reduced levels of VLCFAs (3−5-fold, Figure 1A, Table S1), and activation of the necroptotic pathway in these cells resulted in significantly less cell death as compared to shRFP cells (Figure 1B, cell viability increased from 21% to 60% with shELOVL7), whereas ELOVL7 knockdown had no effect on cell viability during apoptosis (Figure S1). Moreover, these cells were protected from membrane permeabilization, as indicated by propidium iodide uptake (Figure 1C). These results strongly support the critical role of fatty acid elongation in necroptotic cell death and membrane permeabilization.

ELOVL7 Overexpression Causes Accumulation of VLCFA and Loss of Membrane Integrity. We hypothesized that VLCFA may disrupt cellular membranes due to a mismatch in chain length, since membrane lipids predominantly contain alkyl chains with 16 or 18 carbons.[23,24] In order to study the effects of VLCFA accumulation on membrane permeabilization, we transiently overexpressed C-terminus GFP tagged ELOVL7 (GFP-ELOVL7) in HEK-293T cells. This overexpression did not activate apoptotic or necroptotic pathways (Figure S2A) and allowed us to achieve high cellular concentrations of VLCFA. At 48 h post-transfection, approximately 30−40% of the cells overexpressed ELOVL7 based on GFP signal. In the total cell population, VLCFA accumulated between 2- and 30-fold; in particular, saturated VLCFA C22:0 and C24:0 showed pronounced accumulations (Figure 1D and Table S2).

We next assessed the plasma membrane permeability of cells overexpressing GFP-ELOVL7 by measuring the uptake of propidium iodide (PI) using flow cytometry. We used a plasmid that encodes a fluorescent fusion galactosyltransferase enzyme (commonly used as a Golgi marker) as a negative control, which we refer to as Emerald-Golgi, to test the effect of protein overexpression alone on membrane permeabilization. We specifically investigated the PI uptake of GFP- or Emerald-positive cells. We found that significantly more ELOVL7-overexpressing cells were PI-positive (PI^+) compared to cells that were untransfected or transfected with the control plasmid (Figure 1E). We note that expression of the control plasmid was considerably higher than for ELOVL7, likely contributing to the modest increase in PI^+ cells compared to untransfected controls (data not shown).

Although HEK-293T cells are unlikely to be susceptible to membrane permeabilization through the canonical RIP1-RIP3-MLKL axis due to low expression of RIP3,[25] we further excluded the involvement of this pathway by overexpressing ELOVL7 in cells treated with RIP1 inhibitor Necrostatin-1s or in cells where MLKL was silenced by shRNA. Neither prevented the increase in PI^+ positive cells resulting from ELOVL7 overexpression (Figure S2B,C). Overall, these results show that ELOVL7 overexpression results in the accumulation of VLCFAs and causes plasma membrane permeabilization, independently of the RIP1-RIP3-MLKL axis. These findings are in accordance with our previous work, which showed that VLCFA accumulation occurs downstream of RIP1 activity during necroptosis,[16] indicating that these molecules do not initiate necroptotic signaling but cause membrane permeabilization through a divergent mechanism.

VLCFA Directly Permeabilize Liposomes. Our results establish the activity of ELOVL7 as an important mediator of membrane integrity. We next sought to address if VLCFA directly permeabilizes membranes. Since we observed that the overexpression of ELOVL7 also increased the levels of phospholipids such as phosphatidylcholines (Figure S2D), we aimed to avoid the processing of VLCFAs by the cellular machinery and their attachment to other biomolecules by using a cell-free system. We employed liposomes as a model system to study the integrity of a lipid bilayer in the presence of increasing concentrations of VLCFA. We prepared calcein-loaded liposomes using DSPC (PC18:0/18:0) and cholesterol (~2:1 molar ratio), two lipids that are abundant in the plasma membrane, and investigated liposome permeability based on calcein release. Using this system, we tested the ability of the VLCFA lignoceric acid (C24:0 FA) vs palmitic acid (C16:0 FA) to permeabilize the liposomes. C16:0 FA did not induce significant membrane permeabilization at concentrations up to 25 μM, whereas C24:0 FA induced significant permeabilization at 5 μM. At higher concentrations, both fatty acids caused a concentration-dependent increase in calcein release, but treatment with C24:0 FA resulted in significantly higher calcein release than C16:0 FA (Figure 2). These findings indicate that saturated VLCFA may permeabilize membranes and have a higher propensity to do so than their long chain fatty acid counterparts.

MD Simulations Provide Insights into Effects of VLCFA on Membrane Bilayers. In order to understand the molecular basis by which VLCFA might cause membrane permeabilization, we employed all-atom MD simulations. Bilayer systems were constructed to reflect the composition of the liposomes. Simulations were conducted for 1.5 μs for a "pure" bilayer with no free FA (at 160:80 DSPC/cholesterol) and for bilayers with C16:0 (C16) or C24:0 (C24) FA added (at 160:80:20 DSPC/cholesterol/FA). Density maps of the systems are provided in Figures S3−S5. A close inspection of the figures reveals a larger tendency of C24 FA to aggregate into small clusters, whereas C16 FA disperses over the course of the simulation.

DOI: 10.1021/acschembio.9b00616
ACS Chem. Biol. 2019, 14, 2286−2294

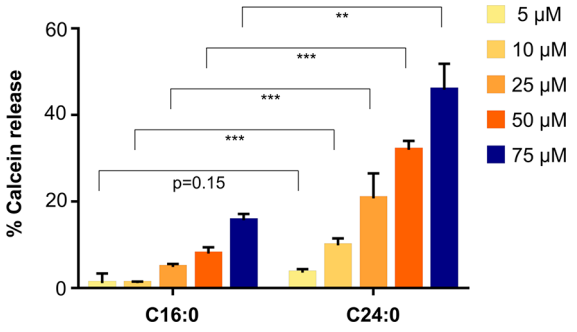

Figure 2. Interaction of C24 FA and C16 FA with bilayers. VLCFA permeabilizes liposomes. Liposome permeabilization was evaluated based on increased fluorescence due to calcein release. Calcein release is expressed as a percent relative to maximum permeabilization caused by detergent, as described in the Materials and Methods. Error bars represent 1 SD; $n = 3$. $^{**}p < 0.01$; $^{***}p < 0.001$.

Hydrogen bond analysis (Table S3 and Figure S6) shows that the addition of either FA has no effect on the cholesterol–water hydrogen bonds. However, the number of cholesterol–DSPC hydrogen bonds decreases slightly upon the addition of either FA. C16 FA forms on average two more hydrogen bonds with cholesterol than C24 FA (6 vs 4), while C24 FA makes a slightly larger number of hydrogen bonds with water (55 vs 52). The small changes in hydrogen bonding and the different and mismatching hydrophobic lengths of the FAs with respect to DSPC results in the cholesterol molecules moving closer to the surface of the bilayer in the case of C24 FA and deeper inside the bilayer when C16 FA is present (Table S4). Although the differences in hydrogen bonding are not large, they are systematic. As has been seen, for example, in the context of liposomes,[26] lipid membranes,[27−29] and water and small molecules,[30,31] systematic differences often lead to profound effects. Here, changes in the position of cholesterol and the different hydrophobic lengths of the FAs lead to changes at the water–bilayer interface. In particular, the addition of C24 FA reduces the number of DSPC–water hydrogen bonds. This is also reflected in the solvent accessible surface area (SASA) for cholesterol, which is slightly larger (393.2 nm^2) for the bilayer–C24 FA in comparison with the bilayer–C16 FA system (390.6 nm^2). Similarly, DSPC is more solvent accessible in the presence of C24 (604.1 nm^2) than C16 (579.9 nm^2). Given that the number of DSPC–water

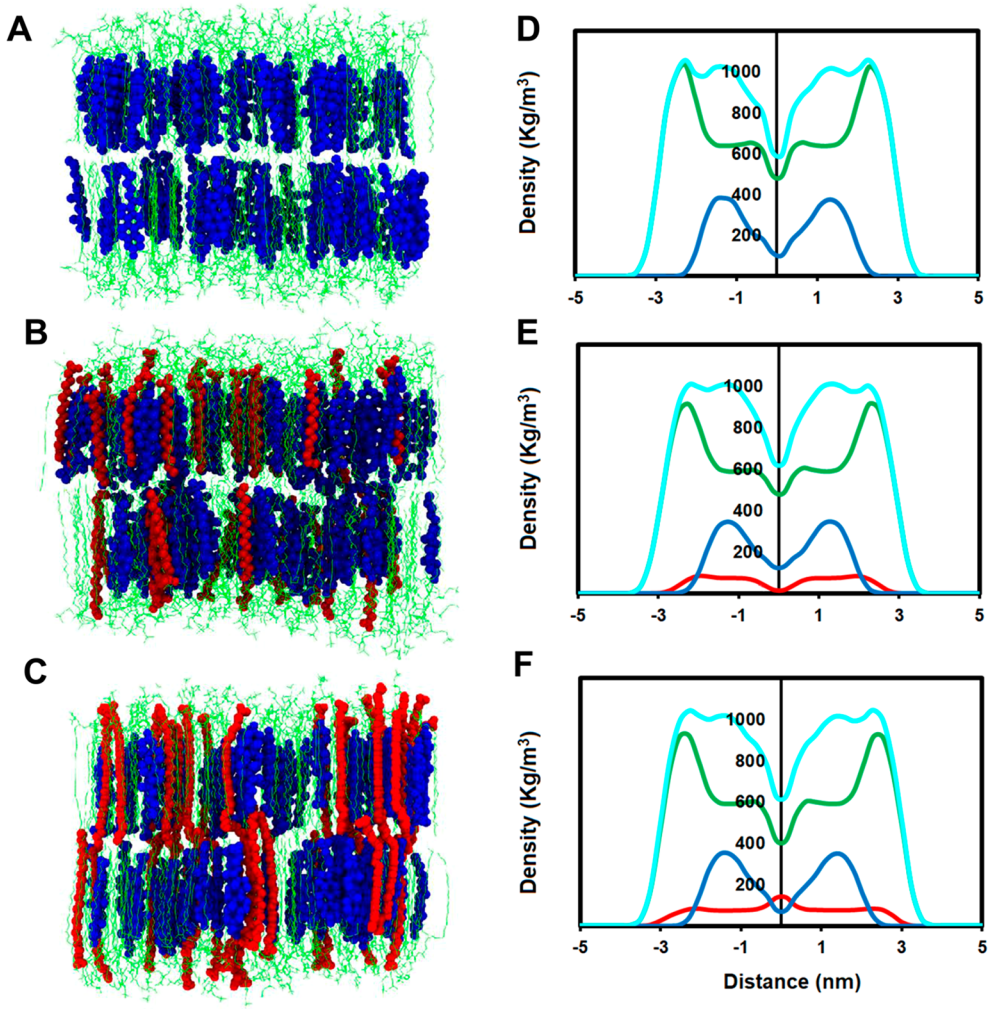

Figure 3. FA alteration of the profile of the lipid bilayer. (A–C) Snapshots at the end of the simulations: (A) pure bilayer, (B) bilayer-C16 FA, and (C) bilayer-C24 FA system. DSPC is shown in green, cholesterol in blue, and FA in red. (D–F) Density profile of (D) pure bilayer, (E) bilayer-C16 FA, and (F) bilayer-C24 FA systems along the *z*-axis (bilayer normal). DSPC is shown in green, cholesterol in blue, FA in red, and total in cyan.

DOI: 10.1021/acschembio.9b00616
ACS Chem. Biol. 2019, 14, 2286–2294

hydrogen bonds decreases upon addition of C24, the increase in SASA appears counterintuitive. This reduction is, however, due to the fact the C24 FA resides closer to the membrane surface and flanks DSPCs' carbonyl and, albeit to a lesser extent, phosphate groups from water (Figure 3).

One of the most striking features of the bilayer−C24 FA system was the interdigitation of the C24 FA chain into the opposite leaflet of the bilayer (Figure 3A,D pure bilayer; B,E bilayer−C16 FA; C,F bilayer−C24 FA). We were interested to determine how this interdigitation might influence the fluidity of the bilayer. We therefore measured the deuterium order parameters (S_{CD}) for the FA and DSPC hydrocarbon chains. Figure 4A shows S_{CD} for the two FAs. Ordering near the head

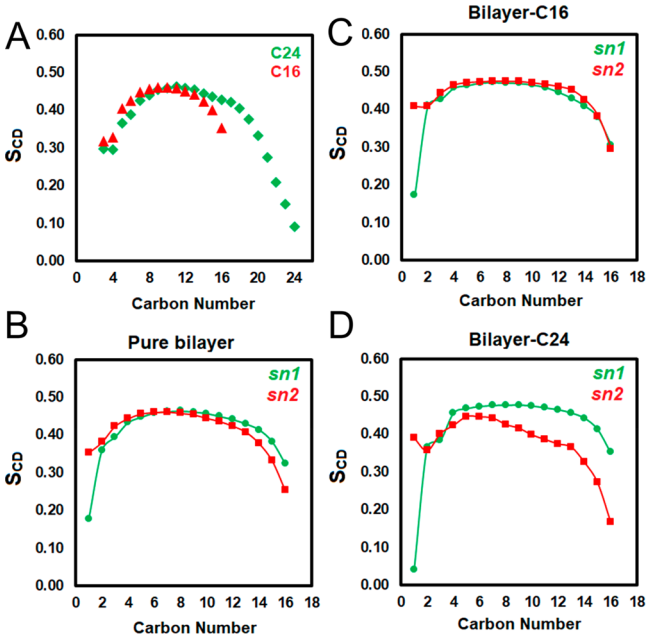

Figure 4. Deuterium order parameters (S_{CD}) from MD simulations. (A–D) S_{CD} for (A) C16 FA (red), C24 FA (green), and DSPC chains (*sn1*, green; *sn2*, red) in (B) pure bilayer, (C) bilayer−C16 FA, and (D) bilayer−C24 FA. The order parameter is defined as $S_{CD} = \langle(3 \cos \theta_n - 1)/2\rangle$, where θ_n is the angle between the *n*th segmental vector along the hydrocarbon chain and the bilayer normal; the brackets stand for averaging.

is very similar; however, the chain ends behave differently with C24 FA being significantly disordered. Figure 4B shows the DPSC order parameters for the two alkyl chains in the absence of added FA. While neither FA has a significant effect on the sn1 chain, the presence of FA does affect the order parameter of the sn2 chain. Figure 4C shows that in the presence of C16 FA, the sn2 chain becomes more ordered. The presence of C24 FA (Figure 4D) has an opposite effect. C24 FA makes the chain disordered, with the effect becoming stronger toward the end of the chain. Importantly, a loss of chain order is required for increased fluidity,[32−34] and thus the higher permeability of the C24 FA system may be a result of the lower chain order.

At the center of the bilayer, the density of bilayer components changes for different systems. Specifically, total density of the bilayer at the center is ∼531, 595, and 591 kg/m^3 for pure bilayer (Figure 3D), bilayer−C16 FA (Figure 3E), and bilayer−C24 FA (Figure 3F) systems, respectively. As is seen in Figure 3F, the density of DSPC and cholesterol at the center is the smallest for the bilayer−C24 FA system. Of particular interest is the density of FA at the center, which shows a minimum for C16 FA (∼15 kg/m^3) and a maximum for C24 FA (∼145 kg/m^3).

The increase in the density at the bilayer center observed for bilayer−C16 FA is partly due to the presence of palmitic acid tails and partly due to the deeper position of cholesterols in the bilayer. Although the expectation might be to see a larger increase for C24 FA, this is not the case, likely due to the elongation of the bilayer along the *z* axis, which in turn decreases the density of DSPC and cholesterol at the center (Figure 3E,F).

The different effects of C16 and C24 FAs on the DSPC order parameter, packing pattern of the bilayer, relative position of cholesterol along the *z* axis (normal of the bilayer), the bilayer density profile, hydrogen bonding interactions, and solvent accessibility of the bilayer components collectively determine the relative permeability of the bilayer in the presence of each FA. In particular, the pronounced disorder caused by the presence of C24 FA, especially in the bilayer core, seems a likely culprit for the higher propensity of C24 FA to induce membrane permeabilization.

***In Vitro* Protein Acylation by VLCFAs.** Overall, these results suggest that interaction of VLCFAs with membranes may disrupt membrane integrity at high concentrations. The accumulation of VLCFAs during necroptosis is modest with respect to the concentrations that are needed to permeabilize liposomes (Figure 2). As such, it is possible that VLCFAs are targeted to defined domains, which results in high local concentrations on the plasma membrane.

One way in which fatty acids can participate in membrane-associated signaling events is *via* protein acylation. Covalent modification of a protein with a fatty acid can target cytosolic proteins to membranes or may alter the function, localization, and interactions of proteins which are membrane-associated (reviewed in refs 10, 11). Protein acylation is essential for many signaling processes, including cell division and cell death.[35,36] Translocation of phosphorylated mixed lineage kinase domain-like protein (pMLKL) oligomers from the cytosol to the membrane is crucial to necroptosis,[37] which is driven by electrostatic interactions between positively charged regions of pMLKL and negatively charged phosphatidylinositol phosphate-rich membrane domains.[38] The membrane association of other factors may also be involved. We therefore hypothesized that protein acylation, in particular by VLCFA, may contribute to such interactions dependent on membrane targeting and therefore may be involved in membrane permeabilization during necroptosis.

The most studied modifications by saturated fatty acids are *S*-palmitoylation and *N*-myristoylation. These processes have been traditionally investigated by acyl exchange methods and radioactive probes, but the field has expanded greatly with the development of ω-alkynyl fatty acids. These ω-alkynyl fatty acids can be taken up by cells *in vitro* and conjugated to various reporters via copper(I)-catalyzed azide−alkyne cycloaddition (CuAAC).[39] Various medium (ex. C10) and long chain (ex. C14, C16, C18) ω-alkynyl fatty acid probes have been demonstrated to acylate proteins using this method.[40,41] Thinon et al. have also designed various Δ^9 cis unsaturated ω-alkynyl fatty acids, including one containing 20 carbons, and have shown that these probes were incorporated to various proteins in cells with saturated probes such as C16 and C18 generally preferred as substrates for S-acylation.[40] Using similar azide-based probes, a study investigated the acyl chain

DOI: 10.1021/acschembio.9b00616
ACS Chem. Biol. 2019, 14, 2286−2294

Scheme 1. Synthesis of ω-Alkynyl C20:0 and C22:0 Fatty Acids

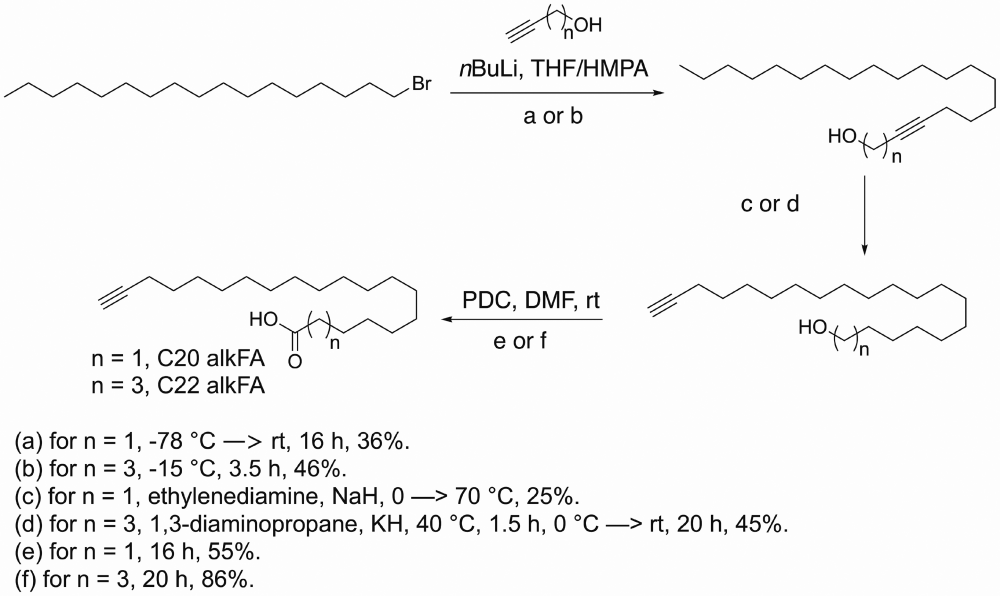

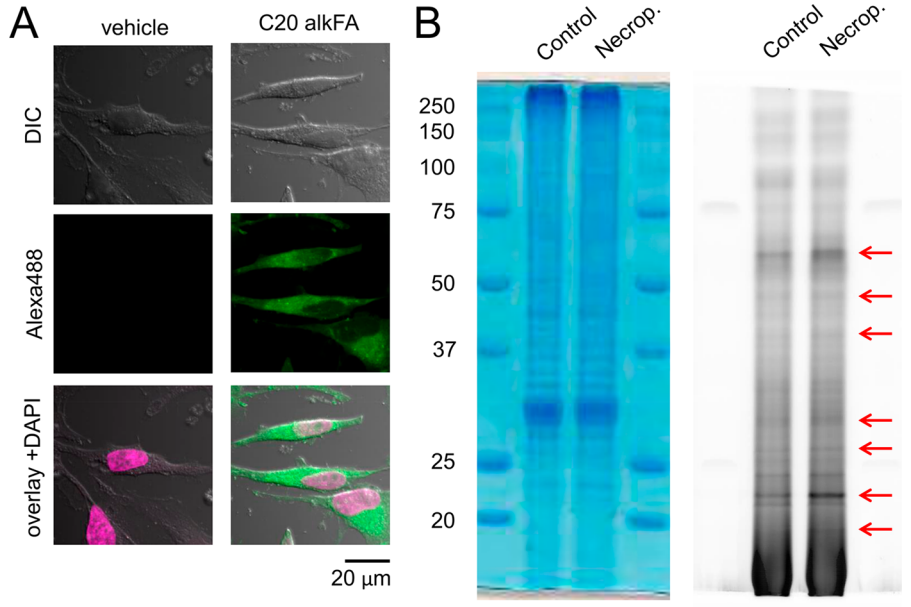

Figure 5. VLCFA acylate proteins. (A) C20 alkFA is uptaken and distributed throughout cells. HeLa cells were treated for 3 h with vehicle or C20 alkFA. Cells were fixed, and alkFA was labeled with Alexa488-azide via CuAAC. (B) C20 alkFA is used as a substrate for protein acylation. Control and necroptotic cells treated with C20 alkFA were membrane fractionated then subjected to CuAAC with Alexa488-azide. The in-gel fluorescence corresponding to labeled proteins is shown in the right panel. Red arrows highlight bands of interest, which show higher levels of protein acylated by C20 alkFA during necroptosis. Coomassie total protein stain is shown in the left panel.

specificity of zinc finger DHHC domain containing enzymes and interactions that govern acyl chain preference.[42]

On the basis of these studies, we aimed to investigate protein fatty acylation by saturated VLCFAs during necroptosis. We initially tested the delivery of various VLCFAs and observed that C24:0 FA showed poor uptake. Instead, we focused on C20:0 FA, which also accumulates with ELOVL7 overexpression (Figure 1C). Adopting previous protocols developed for fatty acid analogs,[42−44] we synthesized ω-alkynyl C20:0 FA (hereafter referred to as C20 alkFA, Scheme 1). Using these probe, we studied protein acylation by VLCFAs in general and during necroptosis.

We first evaluated the uptake and distribution of the probe by fluorescence microscopy. We chose a 3 h treatment based on previous time course studies with similar FA probes.[45] Cells plated on glass coverslips were treated with C20 alkFA complexed with BSA. Cells were washed and fixed then subjected to CuAAC with Alexa488-azide. After additional washing steps, cells were mounted on slides and imaged by fluorescence microscopy. As shown in Figure 5A, fatty acid was uptaken within 3 h of treatment and appeared to be widely distributed throughout the cell.

We then evaluated the utilization of the probe as a substrate for protein acylation. This is commonly accomplished by

DOI: 10.1021/acschembio.9b00616
ACS Chem. Biol. 2019, 14, 2286−2294

taking lysates of cells treated with alkFA and reacting via CuAAC with an azido-fluorophore. The labeled proteins are separated by SDS-PAGE, and in-gel fluorescence can be visualized. On the basis of previous protocols,[45,46] we reasoned that membrane fractionation and solubilization might make the probe more accessible, so we tested the effect of performing the CuAAC in the membrane fraction only vs in the total cell lysate. Indeed, we found that performing membrane fractionation enhanced labeling (Figure S7A). Next, we compared the performance of the C20 alkFA probe to the well-established C16 alkFA probe. Qualitatively, these probes appear to have similar labeling patterns (Figure S7B), as does a longer C22 alkFA (Scheme 1, Figure S7C) that mimics C22 FA, a VLCFA that shows significant accumulation during necroptosis.[16] Hydroxylamine treatment significantly reduces labeling, suggesting S-linkages constitute the majority of the acylation we observe (Figure S7B). Furthermore, we observed that during necroptosis the C20 alkFA probe exhibits a similar overall labeling pattern (Figure 5B).

We envision that proteins which are increasingly acylated (in particular by VLCFAs) during necroptosis may be targeted to membrane domains, which may mediate their function and ultimately contribute to membrane permeabilization. We have highlighted several bands of interest (red arrows in Figure 5B) which indicate increased levels of specific acylated proteins. These differences are not merely due to differences in uptake between control and necroptotic cells (Figure S8). It is possible that these and other proteins (which may be lower in abundance or insufficiently resolved by SDS-PAGE) are involved in membrane permeabilization during necroptosis. Next, we tested whether MLKL and pMLKL could be targets for fatty acylation by VLCFAs based on the involvement of pMLKL in membrane permeabilization during necroptosis. We analyzed the protein content by Western blotting and did not observe detectable levels of MLKL and pMLKL in the neutravidin enriched portion (Figure S9). This is consistent with phosphatidyl inositol phosphate-dependent recruitment of pMLKL to the plasma membrane.[37,38]

Finally, we used a perturbation-based approach to provide links between protein fatty acylation and necroptosis. Due to the redundancy of different acyltransferases, we used a small molecule inhibitor that targets DHHC-mediated transfer, Compound V (Figure S10A). Although the potency and specificity of Compound V has only been investigated in limited *in vitro* systems,[47,48] we chose to use this inhibitor since it is more likely to avoid off-target effects on fatty acid-processing enzymes. We observed that after induction of necroptosis, cells pretreated with Compound V showed a modest (>10%) increase in cell viability (Figure S10B, p = 0.0005). We note that Compound V alone induces toxicity under these conditions, and if we scale the viability of Compound V treated cells to 100%, the Compound V-mediated rescue becomes more pronounced (30% increase). In contrast, Compound V did not increase cell viability during apoptosis (Figure S10C). Concurrently, if DHHC-mediated acyl-CoA transfer is involved in the execution of necroptotic cell death, then inhibiting acyl-CoA synthetase activity should also prevent cell death. We find that pretreatment with Triacsin C (inhibitor of long-chain fatty acyl CoA synthetase)[49,50] resulted in a significant increase in cell viability during necroptosis, suggesting that activation of fatty acids is indeed involved in necroptosis (Figure S10D). However, based on the modest rescue in cell death in the presence of Compound V, the involvement of other mechanisms or cellular fatty acylation pathways during necroptosis seems likely.

CONCLUSION

It has long been known that the fatty acyl composition of lipids has a large effect on the biophysical properties of membranes.[8,51] A recent study by Shen *et al.* demonstrated that palmitic acid influences the phase behavior and function of the endoplasmic reticulum by causing solid-like domain separation in the fluidic endoplasmic reticulum membrane.[15] We are just beginning to understand how different lipids are trafficked to cellular membranes, how they interact with other membrane components, and how they are maintained at particular membrane sites in the cellular context. In addition to the phenotypes and physiological effects related to oxidation of unsaturated lipids,[13,52] studies have shown the involvement of distinct lipid species in the maintenance of cellular homeostasis and fundamental cellular processes.[14]

In this work, we investigated the role of saturated VLCFAs during necroptosis. We established that targeted perturbations to increase the cellular pools of VLCFAs that accumulate during necroptosis significantly impairs membrane integrity. We show that C24 FA permeabilizes liposomes more readily than C16 FA, suggesting that VLCFAs themselves, rather than other lipids that contain these acyl chains, can mediate membrane disruption. MD simulations suggest that the interdigitation of VLCFAs between leaflets of the membrane bilayer can facilitate the membrane disruption we observe in liposomes in the presence of VLCFAs. It has been suggested that saturated phospholipids cluster together with cholesterol based on *in vitro* findings.[53] Furthermore, association with cholesterol-rich components of the cellular membranes can affect protein and membrane trafficking.[53−55] As such, it is tempting to propose that VLCFAs might closely associate with membrane cholesterols and accumulate at cholesterol-rich regions of cellular membranes.

One intriguing observation was that high concentrations of FA are needed to permeabilize liposome bilayers (Figure 2), which greatly exceed the intracellular saturated VLCFA increases we observed during necroptosis. As such, we envisioned that incorporation of VLCFAs into proteins can facilitate their recruitment to lipid domains and thereby achieve high local concentrations in cellular membranes. Although not completely understood, acylation by VLCFAs has recently been demonstrated in two systems.[42,43] On the basis of this, we synthesized a C20 alkFA and showed its incorporation to proteins during necroptosis. Our results demonstrate that saturated VLCFAs can directly modify many proteins, which presents potential links to membrane permeabilization and its inflammatory consequences *in vivo*. Consistent with a recent study in HEK-293T cells,[42] the acylation we observe appears to be *S*-linked. Taken together, these results point to multiple potential mechanisms of membrane disruption by VLCFAs during necroptosis, either by direct permeabilization via bilayer disruption or targeting of VLCFA-acylated proteins. Much exciting work remains on investigating the mechanisms and protein machinery that are responsible for protein fatty acylation by saturated VLCFAs and the implication of this type of fatty acylation on membrane permeabilization during necroptosis.

DOI: 10.1021/acschembio.9b00616
ACS Chem. Biol. 2019, 14, 2286−2294

■ ASSOCIATED CONTENT

Supporting Information

The Supporting Information is available free of charge on the ACS Publications website at DOI: 10.1021/acschembio.9b00616.

Four tables, 10 figures, ^{1}H NMR and ^{13}C NMR spectra of compounds synthesized, materials, and additional experimental methods (PDF)

■ AUTHOR INFORMATION

Corresponding Author

*E-mail: ekinatil@buffalo.edu.

ORCID

Laura R. Parisi: 0000-0003-4868-1426
Shahin Sowlati-Hashjin: 0000-0001-6968-1535
Jonathan F. Lovell: 0000-0002-9052-884X
Sherry R. Chemler: 0000-0001-6702-5032
Mikko Karttunen: 0000-0002-8626-3033
G. Ekin Atilla-Gokcumen: 0000-0002-7132-3873

Notes

The authors declare no competing financial interest.

■ ACKNOWLEDGMENTS

We acknowledge the support from the National Science Foundation grant (MCB1817468 to G.E.A.-G. and 1555220 to J.F.L.), the National Institutes of Health (R01EB017270 and DP5OD017898 to J.F.L. and GM078383 to S.R.C.), and the Research Foundation for The State University of New York (J. Solo funds to G.E.A.-G.). M.K. thanks the Natural Sciences and Engineering Research Council of Canada (NSERC) and the Canada Research Chairs Program. Computing facilities were provided by SHARCNET (www.sharcnet.ca) and Compute Canada (www.computecanada.ca). L.R.P. is a recipient of a Speyer Fellowship (UB, Department of Chemistry). We thank D. Lu and S. Fernando for their assistance in cell viability measurements. We thank H. Hang (Rockefeller University) and B. Martin (University of Michigan) for helpful discussions on the use of clickable fatty acids. We also thank S. Cologna (UIC) for providing feedback on our manuscript, A. Siegel (UB North Campus Imaging Facility) for confocal image acquisition, UB Department of Chemical and Biological Engineering for flow cytometer usage, and P. Gollnick (UB Biological Sciences) for ultracentrifuge usage.

■ REFERENCES

(1) van Meer, G., Voelker, D. R., and Feigenson, G. W. (2008) Membrane lipids: where they are and how they behave. *Nat. Rev. Mol. Cell Biol. 9*, 112−124.

(2) Storck, E. M., Özbalci, C., and Eggert, U. S. (2018) Lipid Cell Biology: A Focus on Lipids in Cell Division. *Annu. Rev. Biochem. 87*, 839−869.

(3) Finkelstein, J., Heemels, M.-T., Shadan, S., and Weiss, U. (2014) Lipids in health and disease. *Nature 510*, 47.

(4) Wymann, M. P., and Schneiter, R. (2008) Lipid signalling in disease. *Nat. Rev. Mol. Cell Biol. 9*, 162−176.

(5) Brügger, B. (2014) Lipidomics: Analysis of the Lipid Composition of Cells and Subcellular Organelles by Electrospray Ionization Mass Spectrometry. *Annu. Rev. Biochem. 83*, 79−98.

(6) Peng, B., Geue, S., Coman, C., Münzer, P., Kopczynski, D., Has, C., Hoffmann, N., Manke, M.-C., Lang, F., Sickmann, A., Gawaz, M., Borst, O., and Ahrends, R. (2018) Identification of key lipids critical for platelet activation by comprehensive analysis of the platelet lipidome. *Blood 132*, e1−e12.

(7) Kimura, T., Jennings, W., and Epand, R. M. (2016) Roles of specific lipid species in the cell and their molecular mechanism. *Prog. Lipid Res. 62*, 75−92.

(8) Tsubone, T. M., Junqueira, H. C., Baptista, M. S., and Itri, R. (2019) Contrasting roles of oxidized lipids in modulating membrane microdomains. *Biochim. Biophys. Acta, Biomembr. 1861*, 660−669.

(9) Jump, D. B. (2009) Mammalian fatty acid elongases. *Methods Mol. Biol. 579*, 375−389.

(10) Lanyon-Hogg, T., Faronato, M., Serwa, R. A., and Tate, E. W. (2017) Dynamic Protein Acylation: New Substrates, Mechanisms, and Drug Targets. *Trends Biochem. Sci. 42*, 566−581.

(11) Chamberlain, L. H., and Shipston, M. J. (2015) The physiology of protein S-acylation. *Physiol. Rev. 95*, 341−376.

(12) Magtanong, L., Ko, P. J., and Dixon, S. J. (2016) Emerging roles for lipids in non-apoptotic cell death. *Cell Death Differ. 23*, 1099−1109.

(13) Magtanong, L., Ko, P. J., To, M., Cao, J. Y., Forcina, G. C., Tarangelo, A., Ward, C. C., Cho, K., Patti, G. J., Nomura, D. K., Olzmann, J. A., and Dixon, S. J. (2019) Exogenous Monounsaturated Fatty Acids Promote a Ferroptosis-Resistant Cell State. *Cell Chem. Biol. 26*, 420−432.e9.

(14) Rumora, A. E., LoGrasso, G., Haidar, J. A., Dolkowski, J. J., Lentz, S. I., and Feldman, E. L. (2019) Chain length of saturated fatty acids regulates mitochondrial trafficking and function in sensory neurons. *J. Lipid Res. 60*, 58−70.

(15) Shen, Y., Zhao, Z., Zhang, L., Shi, L., Shahriar, S., Chan, R. B., Di Paolo, G., and Min, W. (2017) Metabolic activity induces membrane phase separation in endoplasmic reticulum. *Proc. Natl. Acad. Sci. U. S. A. 114*, 13394−13399.

(16) Parisi, L. R., Li, N., and Atilla-Gokcumen, G. E. (2017) Very Long Chain Fatty Acids Are Functionally Involved in Necroptosis. *Cell Chem. Biol. 24*, 1445−1454.e8.

(17) Degterev, A., Huang, Z., Boyce, M., Li, Y., Jagtap, P., Mizushima, N., Cuny, G. D., Mitchison, T. J., Moskowitz, M. A., and Yuan, J. (2013) Chemical inhibitor of nonapoptotic cell death with therapeutic potential for ischemic brain injury. *Nat. Chem. Biol. 9*, 112−119.

(18) Weinlich, R., Oberst, A., Beere, H. M., and Green, D. R. (2017) Necroptosis in development, inflammation and disease. *Nat. Rev. Mol. Cell Biol. 18*, 127−136.

(19) Kaczmarek, A., Vandenabeele, P., and Krysko, D. V. (2013) Necroptosis: the release of damage-associated molecular patterns and its physiological relevance. *Immunity 38*, 209−223.

(20) Ohno, Y., Suto, S., Yamanaka, M., Mizutani, Y., Mitsutake, S., Igarashi, Y., Sassa, T., and Kihara, A. (2010) ELOVL1 production of C24 acyl-CoAs is linked to C24 sphingolipid synthesis. *Proc. Natl. Acad. Sci. U. S. A. 107*, 18439−18444.

(21) Tamura, K., Makino, A., Hullin-Matsuda, F., Kobayashi, T., Furihata, M., Chung, S., Ashida, S., Miki, T., Fujioka, T., Shuin, T., Nakamura, Y., and Nakagawa, H. (2009) Novel lipogenic enzyme ELOVL7 is involved in prostate cancer growth through saturated long-chain fatty acid metabolism. *Cancer Res. 69*, 8133−8140.

(22) Purdy, J. G., Shenk, T., and Rabinowitz, J. D. (2015) Fatty acid elongase 7 catalyzes the lipidome remodeling essential for human cytomegalovirus replication. *Cell Rep. 10*, 1375−1385.

(23) Dawaliby, R., Trubbia, C., Delporte, C., Noyon, C., Ruysschaert, J.-M., Van Antwerpen, P., and Govaerts, C. (2016) Phosphatidylethanolamine Is a Key Regulator of Membrane Fluidity in Eukaryotic Cells. *J. Biol. Chem. 291*, 3658−3667.

(24) van Meer, G., and de Kroon, A. I. (2011) Lipid map of the mammalian cell. *J. Cell Sci. 124*, 5−8.

(25) He, S., Wang, L., Miao, L., Wang, T., Du, F., Zhao, L., and Wang, X. (2009) Receptor Interacting Protein Kinase-3 Determines Cellular Necrotic Response to TNF-α. *Cell 137*, 1100−1111.

(26) Carter, K. A., Shao, S., Hoopes, M. I., Luo, D., Ahsan, B., Grigoryants, V. M., Song, W., Huang, H., Zhang, G., Pandey, R. K., Geng, J., Pfeifer, B. A., Scholes, C. P., Ortega, J., Karttunen, M., and

DOI: 10.1021/acschembio.9b00616
ACS Chem. Biol. 2019, 14, 2286−2294

Lovell, J. F. (2014) Porphyrin−phospholipid liposomes permeabilized by near-infrared light. *Nat. Commun. 5*, 3546.
(27) Seu, K. J., Cambrea, L. R., Everly, R. M., and Hovis, J. S. (2006) Influence of lipid chemistry on membrane fluidity: tail and headgroup interactions. *Biophys. J. 91*, 3727−3735.
(28) Volkov, V. V., Palmer, D. J., and Righini, R. (2007) Distinct Water Species Confined at the Interface of a Phospholipid Membrane. *Phys. Rev. Lett. 99*, 078302.
(29) Elola, M. D., and Rodriguez, J. (2018) Influence of Cholesterol on the Dynamics of Hydration in Phospholipid Bilayers. *J. Phys. Chem. B 122*, 5897−5907.
(30) Eaves, J. D., Loparo, J. J., Fecko, C. J., Roberts, S. T., Tokmakoff, A., and Geissler, P. L. (2005) Hydrogen bonds in liquid water are broken only fleetingly. *Proc. Natl. Acad. Sci. U. S. A. 102*, 13019.
(31) Titantah, J. T., and Karttunen, M. (2015) Crossovers in supercooled solvation water: Effects of hydrophilic and hydrophobic interactions. *Europhys. Lett. 110*, 38006.
(32) Schuler, I., Milon, A., Nakatani, Y., Ourisson, G., Albrecht, A. M., Benveniste, P., and Hartman, M. A. (1991) Differential effects of plant sterols on water permeability and on acyl chain ordering of soybean phosphatidylcholine bilayers. *Proc. Natl. Acad. Sci. U. S. A. 88*, 6926−6930.
(33) Xiang, T. X., and Anderson, B. D. (1997) Permeability of acetic acid across gel and liquid-crystalline lipid bilayers conforms to free-surface-area theory. *Biophys. J. 72*, 223−237.
(34) Xiang, T. X., and Anderson, B. D. (1998) Influence of chain ordering on the selectivity of dipalmitoylphosphatidylcholine bilayer membranes for permeant size and shape. *Biophys. J. 75*, 2658−2671.
(35) Frohlich, M., Dejanovic, B., Kashkar, H., Schwarz, G., and Nussberger, S. (2014) S-palmitoylation represents a novel mechanism regulating the mitochondrial targeting of BAX and initiation of apoptosis. *Cell Death Dis. 5*, No. e1057.
(36) Zhang, M. M., Wu, P. Y., Kelly, F. D., Nurse, P., and Hang, H. C. (2013) Quantitative control of protein S-palmitoylation regulates meiotic entry in fission yeast. *PLoS Biol. 11*, No. e1001597.
(37) Wang, H., Sun, L., Su, L., Rizo, J., Liu, L., Wang, L.-F., Wang, F.-S., and Wang, X. (2014) Mixed lineage kinase domain-like protein MLKL causes necrotic membrane disruption upon phosphorylation by RIP3. *Mol. Cell 54*, 133−146.
(38) Quarato, G., Guy, C. S., Grace, C. R., Llambi, F., Nourse, A., Rodriguez, D. A., Wakefield, R., Frase, S., Moldoveanu, T., and Green, D. R. (2016) Sequential Engagement of Distinct MLKL Phosphatidylinositol−Binding Sites Executes Necroptosis. *Mol. Cell 61*, 589−601.
(39) Thinon, E., and Hang, H. C. (2015) Chemical reporters for exploring protein acylation. *Biochem. Soc. Trans. 43*, 253−261.
(40) Thinon, E., Percher, A., and Hang, H. C. (2016) Bioorthogonal Chemical Reporters for Monitoring Unsaturated Fatty-Acylated Proteins. *ChemBioChem 17*, 1800−1803.
(41) Hannoush, R. N., and Arenas-Ramirez, N. (2009) Imaging the Lipidome: ω-Alkynyl Fatty Acids for Detection and Cellular Visualization of Lipid-Modified Proteins. *ACS Chem. Biol. 4*, 581−587.
(42) Greaves, J., Munro, K. R., Davidson, S. C., Riviere, M., Wojno, J., Smith, T. K., Tomkinson, N. C. O., and Chamberlain, L. H. (2017) Molecular basis of fatty acid selectivity in the zDHHC family of S-acyltransferases revealed by click chemistry. *Proc. Natl. Acad. Sci. U. S. A. 114*, E1365.
(43) Chen, B., Niu, J., Kreuzer, J., Zheng, B., Jarugumilli, G. K., Haas, W., and Wu, X. (2018) Auto-fatty acylation of transcription factor RFX3 regulates ciliogenesis. *Proc. Natl. Acad. Sci. U. S. A. 115*, E8403−E8412.
(44) Lumbroso, A., Abermil, N., and Breit, B. (2012) Atom economic macrolactonization and lactonization viaredox-neutral rhodium-catalyzed coupling of terminal alkynes with carboxylic acids. *Chem. Sci. 3*, 789−793.
(45) Martin, B. R., Wang, C., Adibekian, A., Tully, S. E., and Cravatt, B. F. (2012) Global profiling of dynamic protein palmitoylation. *Nat. Methods 9*, 84−89.
(46) Martin, B. R., and Cravatt, B. F. (2009) Large-scale profiling of protein palmitoylation in mammalian cells. *Nat. Methods 6*, 135−138.
(47) Ducker, C. E., Griffel, L. K., Smith, R. A., Keller, S. N., Zhuang, Y., Xia, Z., Diller, J. D., and Smith, C. D. (2006) Discovery and characterization of inhibitors of human palmitoyl acyltransferases. *Mol. Cancer Ther. 5*, 1647−1659.
(48) Jennings, B. C., Nadolski, M. J., Ling, Y., Baker, M. B., Harrison, M. L., Deschenes, R. J., and Linder, M. E. (2009) 2-Bromopalmitate and 2-(2-hydroxy-5-nitro-benzylidene)-benzo[b]thiophen-3-one inhibit DHHC-mediated palmitoylation in vitro. *J. Lipid Res. 50*, 233−242.
(49) Tomoda, H., Igarashi, K., Cyong, J. C., and Omura, S. (1991) Evidence for an essential role of long chain acyl-CoA synthetase in animal cell proliferation. Inhibition of long chain acyl-CoA synthetase by triacsins caused inhibition of Raji cell proliferation. *J. Biol. Chem. 266*, 4214−4219.
(50) Bando, M., Iwakura, H., Koyama, H., Hosoda, H., Shigematsu, Y., Ariyasu, H., Akamizu, T., Kangawa, K., and Nakao, K. (2016) High incorporation of long-chain fatty acids contributes to the efficient production of acylated ghrelin in ghrelin-producing cells. *FEBS Lett. 590*, 992−1001.
(51) Silvius, J. R., and McElhaney, R. N. (1979) Effects of phospholipid acylchain structure on thermotropic phase properties. 2: Phosphatidylcholines with unsaturated or cyclopropane acyl chains. *Chem. Phys. Lipids 25*, 125−134.
(52) Forcina, G. C., and Dixon, S. J. (2019) GPX4 at the Crossroads of Lipid Homeostasis and Ferroptosis. *Proteomics 19*, 1800311.
(53) Brown, D. A., and London, E. (2000) Structure and Function of Sphingolipid- and Cholesterol-rich Membrane Rafts. *J. Biol. Chem. 275*, 17221−17224.
(54) Busija, A. R., Patel, H. H., and Insel, P. A. (2017) Caveolins and cavins in the trafficking, maturation, and degradation of caveolae: implications for cell physiology. *Am.J. Physiol. Cell Physiol. 312*, C459−C477.
(55) Yang, Z., Qin, W., Chen, Y., Yuan, B., Song, X., Wang, B., Shen, F., Fu, J., and Wang, H. (2018) Cholesterol inhibits hepatocellular carcinoma invasion and metastasis by promoting CD44 localization in lipid rafts. *Cancer Lett. 429*, 66−77.

DOI: 10.1021/acschembio.9b00616
ACS Chem. Biol. 2019, 14, 2286−2294